

Modulation of intrinsic resting-state fMRI networks in women with chronic migraine

X. Michelle Androulakis,
MD
Kaitlin Krebs, MSc
B. Lee Peterlin, DO
Tianming Zhang, BS
Nasim Maleki, PhD
Souvik Sen, MD
Chris Rorden, PhD
Priyantha Herath, MD,
PhD

Correspondence to
Dr. Androulakis:
Michelle.Androulakis@uscmed.sc.edu

ABSTRACT

Objective: To evaluate the intrinsic resting functional connectivity of the default mode network (DMN), salience network (SN), and central executive network (CEN) network in women with chronic migraine (CM), and whether clinical features are associated with such abnormalities.

Methods: We analyzed resting-state connectivity in 29 women with CM as compared to age- and sex-matched controls. Relationships between clinical characteristics and changes in targeted networks connectivity were evaluated using a multivariate linear regression model.

Results: All 3 major intrinsic brain networks were less coherent in CM (DMN: $p = 0.030$, SN: $p = 0.007$, CEN: $p = 0.002$) as compared to controls. When stratified based on medication overuse headache (MOH) status, CM without MOH (DMN: $p = 0.029$, SN: $p = 0.023$, CEN: $p = 0.003$) and CM with MOH (DMN: $p = 0.016$, SN: $p = 0.016$, CEN: $p = 0.015$) were also less coherent as compared to controls. There was no difference in CM with MOH as compared to CM without MOH (DMN: $p = 0.382$, SN: $p = 0.408$, CEN: $p = 0.419$). The frequency of moderate and severe headache days was associated with decreased connectivity in SN ($p = 0.003$) and CEN ($p = 0.015$), while cutaneous allodynia was associated with increased connectivity in SN ($p = 0.011$).

Conclusions: Our results demonstrated decreased overall resting-state functional connectivity of the 3 major intrinsic brain networks in women with CM, and these patterns were associated with frequency of moderate to severe headache and cutaneous allodynia. *Neurology*® 2017;89:163-169

GLOSSARY

ASC = Allodynia Symptom Checklist; **BMI** = body mass index; **BOLD** = blood oxygenation level-dependent; **CEN** = central executive network; **CM** = chronic migraine; **DLPFC** = dorsolateral prefrontal cortex; **DMN** = default mode network; **DSM-IV** = *Diagnostic and Statistical Manual of Mental Disorders, 4th edition*; **EM** = episodic migraine; **FOV** = field of view; **HIT** = Headache Impact Test; **ICHD** = International Classification of Headache Disorders; **IFBN** = intrinsic functional brain networks; **MNI** = Montreal Neurologic Institute; **MOH** = medication overuse headache; **MPRAGE** = magnetization-prepared rapid gradient echo; **PFC** = dorsolateral prefrontal cortex; **PHQ** = Patient Health Questionnaire; **ROI** = region of interest; **rs-fMRI** = resting-state functional MRI; **SN** = salience network; **TE** = echo time; **TI** = inversion time; **VLPPFC** = ventrolateral prefrontal cortex.

The exact pathophysiologic underpinnings of chronic migraine (CM) are unknown. The current understanding suggests an interplay between genetics and environmental risk factors.¹ Given that pain perception has various affective influences, beyond the immediate processing of painful sensations, cortical modulation of the limbic areas may be central in how patients perceive pain.^{2,3} Therefore, a critical question to be answered is how the resting-state functional brain connectivity adapts to the continuous processing and modulation of pain in CM.

Intrinsic functional brain networks (IFBN) such as default mode network (DMN), salience network (SN), and central executive network (CEN) are state-dependent, spatial topographies consisting of functionally correlated brain regions, which may be pathophysiologic surrogates of the neural activities.^{4,5} Previous resting-state functional MRI (rs-fMRI) studies in episodic migraine (EM) have demonstrated atypical focal connectivity within the DMN, SN, and CEN.⁶⁻¹¹ There is a paucity of data on overall rs-fMRI connectivity patterns and association with clinical characteristics in CM interictally. Such an approach to the brain connectivity may be important given that pain awareness is dependent upon a complex array of parallel processes

Supplemental data
at Neurology.org

From the Departments of Neurology (X.M.A., K.K., S.S., P.H.), Statistics (T.Z.), and Psychology (C.R.), University of South Carolina, Columbia; Department of Neurology (B.L.P.), Johns Hopkins University, Baltimore, MD; and Department of Psychiatry (N.M.), Massachusetts General Hospital, Boston.

Go to Neurology.org for full disclosures. Funding information and disclosures deemed relevant by the authors, if any, are provided at the end of the article.

that adapt to representation of internal and external stimuli in real time, instead of passive primary sensory interpretation.¹²

We simultaneously evaluated the 3 IFBN and their relationships with clinical characteristics. We hypothesize that the connectivity in each IFBN will be decreased in CM, and clinical characteristics will be associated with such connectivity abnormalities; in addition, the IFBN may be differentially affected in CM with medication overuse headache (MOH) and without MOH.

METHODS Participants. Women were eligible for the study if they were 18 years or older, met diagnostic criteria fulfilling International Classification of Headache Disorders (ICHD)–III-beta for CM as determined by a headache specialist, or were nonpain, nonheadache controls. CM subgroups were characterized based on medication overuse status (with or without) per ICHD-III-beta diagnostic criteria. Participants were excluded if they had MRI contraindication, neurologic or pain disorders other than CM, any chronic illness (i.e., hypertension, diabetes, hepatic, renal, chronic inflammatory, or infectious disease), or inability to follow study protocol while completing assessments.

All CM participants were age- and sex-matched to healthy controls. Controls were excluded if they had a family history of migraine or used over the counter/prescription pain medication for more than 5 days per month. CM participants were scanned at their baseline level of pain, at least 24 hours outside of their acute pain exacerbation period; any participant who came in within 24 hours of acute pain exacerbation was rescheduled.

All participants underwent vital sign evaluation including body mass index (BMI) and a neurologic examination and completed a standardized questionnaire to ascertain demographics including age, sex, race, and educational level as well as clinical characteristics including (1) duration of migraine history, (2) duration of CM history, (3) family history of migraine, (4) current medications, (5) number of moderate to severe headache days per month, (6) location of migraine, (7) presence of aura, (8) headache-related disability as determined by the Headache Impact Test (HIT-6), (9) depression as determined by the Patient Health Questionnaire (PHQ-9), and (10) allodynia as measured by the Allodynia Symptom Checklist (ASC12).¹³

Headache Impact Test. The HIT-6 is a validated questionnaire that consists of 6 items reflecting quality of life. Higher scores (range 36–78) indicate an increasing effect of headaches on daily functioning.¹⁴

Patient Health Questionnaire. The PHQ-9 is a diagnostic measure for clinical depression. A score of ≥ 15 on the PHQ-9 is associated with a 68% sensitivity and 95% specificity for diagnosing major depressive disorder based on DSM-IV criteria.¹⁵

Standard protocol approvals, registrations, and patient consents. The study protocol was approved by institutional review boards at the University of South Carolina. Written informed consent was obtained from all participants.

MRI. All participants were scanned on a Siemens (Munich, Germany) 3T scanner located at the McCausland Center for Brain Imaging (Columbia, SC). Some participants (5 CM and 5 controls) were scanned prior to a system hardware upgrade;

however, any variance due to this upgrade was controlled for in our analysis by adding this as a nuisance regressor variable to general linear model using the Freedman-Lane approach. (To test any potential influence of including participants scanned prior to system hardware on our findings, we ran the same statistical analysis without these 10 participants and the overall results were still significant [<0.05]). Therefore, we chose to include all participants in the analysis and included the choice of head channel coil as a nuisance variable in the linear regression model.¹⁶) Participants were instructed to keep their eyes closed, stay awake, relax, and think of nothing in particular during the resting-state scan. All conditions and lighting were consistent throughout the entire study for all participants.

The imaging parameters for the Trio (12-channel head coil) system consisted of a 6-minute high-resolution T1-weighted magnetization-prepared rapid gradient echo (MPRAGE) scan (repetition time [TR] 2,250 ms, echo time [TE] 4.15 ms, 192 slices, 50% slice gap, flip angle 9°, voxel size 1.0 mm³, field of view [FOV] 256 mm², iPAT factor of 2, and using a sagittal, ascending, single shot acquisition) and a 15-minute resting-state functional imaging scan using a T2*-weighted blood oxygenation level-dependent (BOLD) contrast-sensitive sequence (TR 1,550 ms, TE 34 ms, 42 slices, 20% slice gap, flip angle 71°, voxel size 2.5 mm³, FOV 215 mm², and using a transversal, descending, interleaved acquisition).

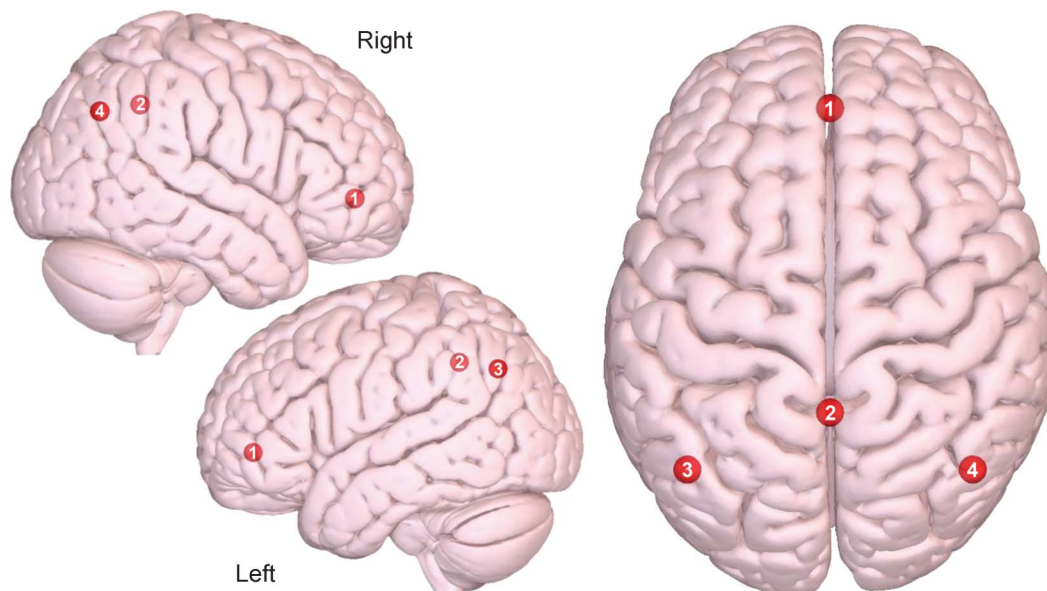
The imaging parameters for the Prisma (20-channel head coil) system included an acquisition of 6-minute high-resolution T1-weighted MPRAGE scan (same parameters as Trio except for TE 4.11 ms) and a 15-minute resting-state functional imaging scan using a T2*-weighted BOLD contrast-sensitive sequence (TR 1,100 ms, TE 35 ms, 56 slices, 20% slice gap, flip angle 72°, voxel size 2.4 × 2.4 × 2.0 mm³, FOV 216 mm², and using a transversal, ascending, interleaved acquisition).

MRI processing. rs-fMRI preprocessing was completed using a combination of Statistical Parametric Mapping 12 (SPM12) software and custom MATLAB scripts. The pipeline consisted of standard procedures including motion correction, coregistration, normalization, frequency filtering (0.01–0.1 Hz bandpass), and spatial smoothing (8 mm full width at half maximum). For each network, a connectivity atlas was constructed using spherical (15 mm diameter) regions of interest (ROIs) centered on the peak Montreal Neurologic Institute (MNI) coordinates for the a priori network of DMN, SN, and CEN.^{17,18} The ROIs and their MNI coordinates used in each network are provided in table e-1 at Neurology.org and illustrated in figures 1–3 and figure e-1.

The DMN included ROIs (nodes) of the lateral parietal, medial prefrontal cortex, and precuneus. The SN includes regions of the dorsolateral prefrontal cortex (PFC), ventrolateral PFC (VLPFC), frontal pole, orbital frontal insula, dorsal anterior cingulate cortex, paracingulate cortex, sublentiform extended amygdala (subcallosal area), supramarginal gyrus, periaqueductal gray area, supplementary motor area/presupplementary motor area, substantia nigra/ventral tegmental area, superior temporal, temporal pole, ventral striatum/pallidum, dorsomedial thalamus, and hypothalamus. The CEN includes regions of the dorsolateral PFC (DLPFC) region of frontal eye fields, dorsal medial PFC, DLPFC, VLPFC, orbital frontoinsula, inferior frontal gyrus, inferior temporal, lateral parietal, anterior thalamus, dorsal caudate, and ventromedial caudate.

Statistical analysis. To create a functional connectivity matrix for each participant, we first extracted the BOLD time series from each ROI that was defined a priori within a network. Then, a functional connectivity matrix (for each separate network) was created using the Pearson correlation coefficient for each pair

Figure 1 Axial and sagittal view of the default mode network

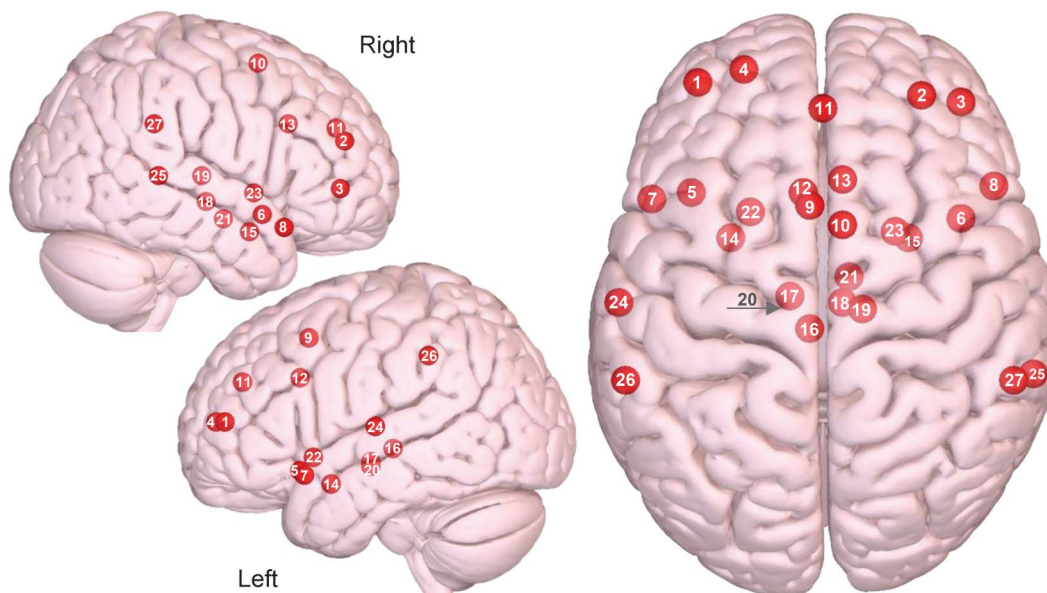


(1) Medial prefrontal, (2) precuneus/posterior cingulate cortex, (3) left lateral parietal, (4) right lateral parietal. Images were made with Surf Ice (nitrc.org/projects/surface/) using the exact Montreal Neurologic Institute coordinate locations and sphere sizes. Node depth is illustrated by transparency.

of ROIs in a network. All Pearson correlation (r) values were then Fisher Z transformed to produce the final functional connectivity matrices (for each participant and each network), which were

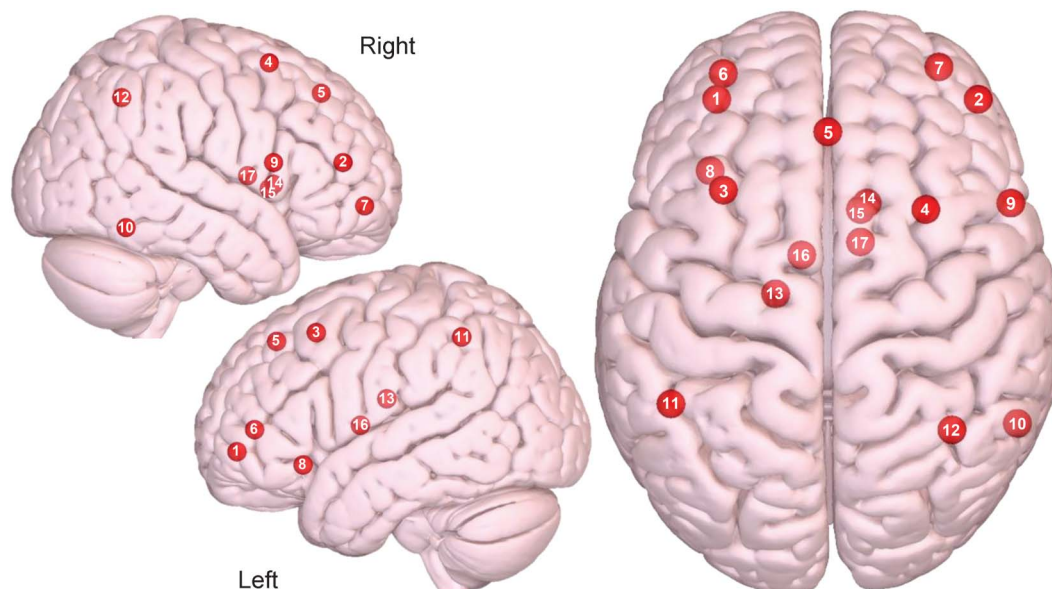
used in the analysis. To investigate the overall functional coherence of a network, the Fisher Z transformed correlation coefficient values between all pairs of ROIs in each network were

Figure 2 Axial and sagittal view of the salience network



(1) Left dorsolateral prefrontal cortex (DLPFC), (2) right DLPFC, (3) right ventrolateral prefrontal cortex, (4) left frontal pole, (5) left orbital frontal insula, (6) right orbital frontal insula, (7) left temporal pole, (8) right temporal pole, (9) left supplementary motor area (SMA)/pre-SMA, (10) right SMA/pre SMA, (11) paracingulate cortex, (12) left dorsal anterior cingulate cortex (dACC), (13) right dACC, (14) left sublentiform extended amygdala, (15) right sublentiform extended amygdala, (16) left periaqueductal gray, (17) left hypothalamus, (18) right hypothalamus, (19) right dorsomedial thalamus, (20) left substantia nigra/ventral tegmental area, (21) right substantia nigra/ventral tegmental area, (22) left ventral striatum/pallidum, (23) right ventral striatum/pallidum, (24) left superior temporal, (25) right superior temporal, (26) left supramarginal gyrus (SMG), (27) right SMG. Images were made with Surf Ice (nitrc.org/projects/surface/) using the exact Montreal Neurologic Institute coordinate locations. Node depth is illustrated by transparency.

Figure 3 Axial and sagittal view of the central executive network



(1) Left dorsolateral prefrontal cortex (DLPFC), (2) right DLPFC, (3) left DLPFC/frontal eye fields (FEF), (4) right DLPFC/FEF, (5) dorsal medial prefrontal cortex, (6) left ventrolateral prefrontal cortex (VLPFC), (7) right VLPFC, (8) left orbital frontal insula, (9) right inferior frontal gyrus, (10) right inferior temporal, (11) left lateral parietal, (12) right lateral parietal, (13) left dorsal caudate, (14) right dorsal caudate, (15) right ventromedial caudate, (16) left anterior thalamus, (17) right anterior thalamus. Images were made with Surf Ice (nitr.org/projects/surface/) using the exact Montreal Neurologic Institute coordinate locations. Node depth is illustrated by transparency.

averaged separately for each participant to obtain the overall network functional connectivity. For each network, a 1-tailed, permuted t test was used to evaluate if there was significant decrease in the overall network connectivity in CM as compared to controls, and a 2-tailed permuted t test was used to determine if differences exist between CM with MOH and CM without MOH. Each statistical test employed a permutation method, using 10,000 permutations, to control for multiple comparisons.¹⁹

To evaluate the relationship between the covariates (clinical features as listed in table 1), we first used a Pearson correlation analysis, χ^2 , and one-way analysis of variance. Subsequently, after removing uncorrelated variables, a multivariate linear regression model was used to determine if any of the clinical features contributed to changes in functional connectivity strength for each network. Confounders, such as age, race, and BMI, were controlled for in this model. Correlations with $p \leq 0.05$ were considered significant (SAS 9.4). In addition, we used a 2-tailed t test to evaluate if there was significant effect on network connectivity in CM participants who used daily migraine preventive medications compared to those who did not.

RESULTS Participants. A total of 56 women were recruited between January 2015 and August 2016 from the University of South Carolina headache clinic. Among the CM participants ($n = 33$), 4 were excluded for motion artifact ($n = 1$), incidental finding on T1 ($n = 2$), and the presence of nonmigraine-related pain during the scan ($n = 1$).

Among the controls ($n = 23$), 4 were excluded for claustrophobia ($n = 2$), motion artifact ($n = 1$), and an incidental finding on T1 ($n = 1$). Individual

characteristics for each group are summarized in table 1 for all participants.

Of the CM participants, 16 had the secondary diagnosis of MOH for the abuse of opioids ($n = 8$), triptans ($n = 9$), combined analgesics ($n = 14$), and combination of triptans with opioids or nonsteroidal anti-inflammatory drugs ($n = 10$). Among 29 CM participants, 15 used daily migraine preventive prophylaxis medications (Topamax or propranolol).

Network differences. In all networks investigated (DMN, SN, and ECN), we found that there was significant decreased overall network connectivity for all CM participants, regardless of MOH status, when compared to controls. Averages and significance values for each CM group and their set of matched controls are listed in table 2. There was no difference between the overall network connectivity strength between CM with MOH when compared to CM without MOH. There were also no differences in overall network connectivity strength of DMN ($p = 0.490$), SN ($p = 0.386$), or CEN ($p = 0.922$) between CM participants who used daily migraine prophylaxis as compared to those who did not.

Clinical characteristics. A multivariate linear regression model was used to analyze the relationship between the overall network connectivity for targeted networks (DMN, SN, and CEN) and clinical characteristics. After adjusting for covariates, we found that

Table 1 Demographics and clinical features of all participants

Demographics for CM and controls	Controls (19)	CM (29)
Age, y ^a	37 ± 11	39 ± 12
Race		
White	12 (63.1)	20 (68.9)
Black	7 (36.9)	9 (31.1)
Highest educational level completed		
Unknown	1 (5.3)	2 (6.9)
High School	4 (21)	7 (24.1)
Undergraduate	10 (52.6)	15 (51.7)
Graduate	4 (21.0)	5 (17.2)
Body mass index ^b	26 ± 5	28 ± 6
Headache features of CM participants		
Headache (moderate to severe) d/mo		18 ± 7
Headache location		
Right		3 (10.4)
Left		5 (17.2)
Bilateral		21 (72.4)
Aura		15 (51.7)
Cranial autonomic symptoms		10 (34.5)
Medication overuse headache		16 (55.2)
Allodynia Score Checklist		6 ± 5
Chronic migraine duration, y		3 ± 2
Migraine history, y		21 ± 12
Family history of migraine		21 (72.4)
Headache Impact Test-6		66 ± 4
Patient Health Questionnaire-9		8 ± 5

Abbreviation: CM = chronic migraine.

Values represent mean ± SD or n (% of total).

^a*p* = 0.591.

^b*p* = 0.153.

number of moderate to severe headache days and allodynia severity were correlated with the SN connectivity strength. For each increase of moderate to severe headache day, the connectivity strength of the SN was predicted to decrease by 0.0094 (*p* = 0.0028). For each increase in allodynia severity (measured by ASC), the connectivity strength of the SN was predicted to increase by 0.0112 (*p* = 0.0111). We also found that the number of moderate to severe headache days per month was negatively correlated with the CEN connectivity strength. For each increase of moderate to severe headache day, the connectivity strength of the CEN was predicted to decrease by 0.0058 (*p* = 0.0147).

In addition, HIT-6 (*p* = 0.3442) and PHQ-9 (*p* = 0.8092) were not correlated with network connectivity changes in the SN and CEN. We did not find any association between any clinical attributes evaluated and connectivity changes in the DMN.

DISCUSSION In this study, focusing on the 3 main IFBN (DMN, SN, and CEN) in the interictal state of CM patients, we found that all 3 IFBN were less coherent, regardless of MOH status. Moreover, we report that 2 of the clinical attributes are closely associated with the changes of the SN and CEN in CM: first, higher headache frequency (moderate to severe) was associated with decreased connectivity strengths in both SN and CEN; second, allodynia severity was associated with increased connectivity in the SN.

Given that a lower correlation within an IFBN implies that the functional components (or nodes) within the network are not oscillating in synchrony, or not following a similar time course, our findings suggest that CM patients have an overall diminished coherence, or functional coactivation, interictally within these important IFBN. Essentially, a change in the time course for at least one or more of the nodes in a network may disrupt the synchrony of the entire network.

In normal human cognition, attention to internal or external stimuli plays a major part in how they become behaviorally relevant. Normally this is how any stimulus is deemed painful, pleasant, neutral, and worthy of a response. This process has 2 ways of dealing with stimuli: a bottom-up filtering process and top-down sensitivity control.²⁰ Filtering and amplification of specific stimuli is thought to occur at multiple hierarchical levels, and at each level, filters may choose those that are of biological importance. As this happens, DMN activity generally fluctuates with SN and CEN activation. In particular, the SN is now thought to be a higher level selection and filtration network for stimuli akin to this.²¹ It has been suggested that this may be how pain captures attention and becomes salient.²² Chronic pain is a complex, multidimensional sensory experience that is a composite of 3 domains: sensory, affective, and cognitive.^{23,24} As CM is a form of chronic pain, susceptibility to this chronic headache disorder would likely occur due to dysfunctional mechanisms that regulate the ways in which these domains react to exogenous and endogenous stimuli.²⁵

Epidemiologic studies have demonstrated that several demographic (age, female sex, lower educational status) and headache-related characteristics, including MOH and cutaneous allodynia, are associated with an increased risk of CM.^{26–28} In our study, allodynia and headache frequency are associated with the connectivity abnormalities. This is suggestive of differential modulations that are simultaneously occurring within the SN and CEN. Specifically, while nodes within SN and CEN are functioning less synchronously with increased headache frequency, certain functional

Table 2 Analysis of overall network connectivity strength

Comparison groups	DMN	SN	CEN
CM vs controls			
Controls	0.59 ± 0.16	0.12 ± 0.11	0.11 ± 0.09
CM	0.50 ± 0.16	0.06 ± 0.12	0.05 ± 0.08
p Value	0.030 ^a	0.007 ^a	0.002 ^a
CM + MOH vs controls			
Controls	0.61 ± 0.15	0.14 ± 0.10	0.13 ± 0.08
CM + MOH	0.51 ± 0.16	0.05 ± 0.13	0.03 ± 0.09
p Value	0.029 ^a	0.023 ^a	0.003 ^a
CM – MOH vs controls			
Controls	0.64 ± 0.13	0.15 ± 0.11	0.14 ± 0.08
CM – MOH	0.50 ± 0.17	0.07 ± 0.11	0.06 ± 0.07
p Value	0.016 ^a	0.016 ^a	0.015 ^a
CM + MOH vs CM – MOH			
p Value	0.382	0.408	0.419

Abbreviations: CEN = central executive network; CM = chronic migraine; DMN = default mode network; MOH = medication overuse headache; SN = salience network.

^aSignificant.

components within the SN are functioning more synchronously as a response, or substrate, to cutaneous allodynia. It is possible that certain segments of the SN may act as a neural surrogate for central sensitization. Taken together, our results suggest that maladaptive networks as reflected by increased or decreased functional coactivation in the SN and CEN might play an essential role in susceptibility to CM.

It is possible that in CM with MOH, excessive use of acute pain medications contributes to downregulation of opioid receptors²⁹ and disrupted addiction/reward dopaminergic pathway,³⁰ which could trigger more widespread disruption to networks, as compared to CM without MOH. Given that there are many unique pairs of intranetwork connections in the DMN, SN, and CEN (6, 136, and 351 respectively), investigation of the intranetwork nodal-to-nodal connectivity would shed light on subtle underpinnings between CM with MOH and CM without MOH, interictally. This work is currently in progress.

Our study has several limitations. First, we cannot be certain that our findings are a consequence of CM or causal. Second, as we did not have a cohort of EM in this study, we cannot generalize to other migraine populations. Third, 15 CM participants were on daily migraine prophylaxis medications; however, further analysis on connectivity changes did not reveal any differences as compared to those who did not take any preventive medication. Fourth, coherence or functional coactivation does not equal electrophysiologic coactivation; this is a limitation

of rs-fMRI methodology. However, rs-fMRI is a valid surrogate for neural activity when no active task is involved.⁵ Finally, participants were not matched according to anxiety/depression scale; therefore we cannot exclude the possibility that some of the changes in connectivity may be related to anxiety/depression. However, using the linear regression model, we did not find PHQ-9 associated with any of the targeted networks' connectivity changes.

We suggest that these intrinsic networks' connectivity may be used as potential biomarkers for the underlying impaired neural networks associated with CM, and as such may have potential as surrogates for evaluating the efficacy of both pharmacologic and nonpharmacologic interventions in CM. We envisage further studies to validate our findings and to refine some of these limitations.

AUTHOR CONTRIBUTIONS

X. Michelle Androulakis: manuscript conception and design, data interpretation, drafting and revising the manuscript for intellectual content, approval of final manuscript. Kaitlin Krebs: study concept and design, acquisition of data, analysis and interpretation of data, critical revision of manuscript for intellectual content. B. Lee Peterlin: study concept and design, analysis and interpretation of data, critical revision of manuscript for intellectual content, approval of final manuscript. Tianming Zhang: analysis and interpretation of data, critical revision of manuscript for intellectual content, approval of final manuscript. Nasim Maleki: critical revision of manuscript for intellectual content, data interpretation, approval of final manuscript. Souvik Sen: critical revision of manuscript for intellectual content, approval of final manuscript. Chris Rorden: critical revision of manuscript for intellectual content, analysis and data interpretation, approval of final manuscript. Priyantha Herath: drafting and revising the manuscript for intellectual content, data interpretation, approval of final manuscript.

ACKNOWLEDGMENT

The authors thank Dr. Todd Schwedt (Mayo Clinic) for assistance with editing the manuscript for intellectual content; Taylor Hanayik (University of South Carolina) for assistance in analysis and interpretation of data; and Viktoriya Duda (University of South Carolina) for acquisition of demographic data.

STUDY FUNDING

Study funded by McCausland Center for Brain Imaging (M-Fund) and University of South Carolina internal grant (ASPIRE II).

DISCLOSURE

X. Androulakis received support from M-fund and ASPIRE grant and funding from TX360. K. Krebs reports no disclosures relevant to the manuscript. B. Peterlin reports funding by NIH/NINDS (grant K23-NS078345) and serves on the editorial board for *Neurology*[®] and as an associate editor for *Headache*. T. Zhang reports no disclosures relevant to the manuscript. N. Maleki reports funding by NIH/NINDS R21 NS099760. S. Sen, C. Rorden, and P. Herath report no disclosures relevant to the manuscript. Go to Neurology.org for full disclosures.

Received December 7, 2016. Accepted in final form April 6, 2017.

REFERENCES

1. May A, Schulte LH. Chronic migraine: risk factors, mechanisms and treatment. *Nat Rev Neurosci* 2016; 12:455–464.

2. Maizels M, Aurora S, Heinricher M. Beyond neurovascular: migraine as a dysfunctional neurolimbic pain network. *Headache* 2012;52:1553–1565.
3. Schwedt TJ, Chiang CC, Chong CD, Dodick DW. Functional MRI of migraine. *Lancet Neurol* 2015;14:81–91.
4. Pizoli CE, Shah MN, Snyder AZ, et al. Resting-state activity in development and maintenance of normal brain function. *Proc Natl Acad Sci USA* 2011;108:11638–11643.
5. Foster BL, He BJ, Honey CJ, Jerbi K, Maier A, Saalman YB. Spontaneous neural dynamics and multi-scale network organization. *Front Syst Neurosci* 2016;10:7.
6. Maleki N, Gollub RL. What have we learned from brain functional connectivity studies in migraine headache. *Headache* 2016;56:453–461.
7. Schwedt TJ, Schlaggar BL, Mar S, et al. Atypical resting-state functional connectivity of affective pain regions in chronic migraine. *Headache* 2013;53:737–751.
8. Schwedt TJ, Chong CD. Functional imaging and migraine: new connections. *Curr Opin Neurol* 2015;28:265–270.
9. Tessitore A, Russo A, Conte F, et al. Abnormal connectivity within executive resting-state network in migraine with aura. *Headache* 2015;55:794–805.
10. Ting X, Kai Y, Ling Z, et al. Intrinsic brain network abnormalities in migraines without aura revealed in resting-state fMRI. *PLoS One* 2012;7:e52927.
11. Amin FM, Hougaard A, Magon S, et al. Change in brain network connectivity during PACAP38-induced migraine attacks: a resting-state functional MRI study. *Neurology* 2016;86:180–187.
12. Chapman CR, Nakamura Y, Flores LY. A constructivist framework for understanding individual differences in pain. *Individual Differences Conscious Experience* 2000; 20:17.
13. Lipton RB, Bigal ME, Ashina S, et al. Cutaneous allodynia in the migraine population. *Ann Neurol* 2008;63:148–158.
14. Kosinski M, Bayliss MS, Bjorner JB, et al. A six-item short-form survey for measuring headache impact: the HIT-6. *Qual Life Res* 2003;12:963–974.
15. Kroenke K, Spitzer RL, Williams JB. The PHQ-9: validity of a brief depression severity measure. *J Gen Intern Med* 2001;16:606–613.
16. Freedman D, Lane D. A nonstochastic interpretation of reported significance levels. *J Bus Econ Stat* 1983;1:292–298.
17. Fox MD, Snyder AZ, Vincent JL, Corbetta M, Van Essen DC, Raichle ME. The human brain is intrinsically organized into dynamic, anticorrelated functional networks. *Proc Natl Acad Sci USA* 2005;102:9673–9678.
18. Seeley WW, Menon V, Schatzberg AF, et al. Dissociable intrinsic connectivity networks for salience processing and executive control. *J Neurosci* 2007;27:2349–2356.
19. Winkler AM, Ridgway GR, Webster MA, Smith SM, Nichols TE. Permutation inference for the general linear model. *Neuroimage* 2014;92:381–397.
20. Knudsen EI. Fundamental components of attention. *Annu Rev Neurosci* 2007;30:57–78.
21. Menon V, Uddin LQ. Saliency, switching, attention and control: a network model of insula function. *Brain Struct Funct* 2010;214:655–667.
22. Kucyi A, Davis KD. The dynamic pain connectome. *Trends Neurosci* 2015;38:86–95.
23. Melzack R, Casey KL. Sensory, motivational and central control determinants of pain: a new conceptual model. *Skin Senses* 1968:1.
24. Melzack R, Wall PD. Psychophysiology of pain. *Int Anesthesiol Clin* 1970;8:3–34.
25. Cosentino G, Fierro B, Vigneri S, et al. Cyclical changes of cortical excitability and metaplasticity in migraine: evidence from a repetitive transcranial magnetic stimulation study. *Pain* 2014;155:1070–1078.
26. Louter MA, Bosker JE, van Oosterhout WP, et al. Cutaneous allodynia as a predictor of migraine chronification. *Brain* 2013;136:3489–3496.
27. Buse D, Manack A, Serrano D, et al. Headache impact of chronic and episodic migraine: results from the American Migraine Prevalence and Prevention Study. *Headache* 2012;52:3–17.
28. Olesen J, Boussier MG, Diener HC, et al. New appendix criteria open for a broader concept of chronic migraine. *Cephalalgia* 2006;26:742–746.
29. Al-Hasani R, Bruchas MR. Molecular mechanisms of opioid receptor-dependent signaling and behavior. *Anesthesiology* 2011;115:1363–1381.
30. Lüscher C, Malenka RC. Drug-evoked synaptic plasticity in addiction: from molecular changes to circuit remodeling. *Neuron* 2011;69:650–663.



Practice Current: An interactive exchange on controversial topics

Share your own best practices.

Read commentary with expert opinion.

Explore results on an interactive world map.

<http://bit.ly/CPpractice3>

Neurology[®] *Clinical Practice*